Local Utility Powerline Communications in the 3-500 kHz Band: Channel Impairments, Noise, and Standards

Marcel Nassar, *Student Member, IEEE,* Jing Lin, *Student Member, IEEE,*
Yousof Mortazavi, *Student Member, IEEE,* Anand Dabak, *Senior Member, IEEE,*
Il Han Kim, *Member, IEEE,* and Brian L. Evans, *Fellow, IEEE*

Abstract

Future Smart Grid systems will intelligently monitor and control energy flows in order to improve the efficiency and reliability of power delivery. This monitoring and control requires low-delay, highly reliable communication between customers, local utilities and regional utilities. A vital part of future Smart Grids is the two-way communication links between smart meters at the customer sites and a (decentralized) command and control center operated by the local utility. To enable these two-way communication links, narrowband powerline communication (PLC) systems operating in the 3-500 kHz band are attractive because they can be deployed over existing outdoor power lines. Power lines, however, have traditionally been designed for one-directional power delivery and remain hostile environments for communication signal propagation. In this article, we review signal processing approaches to model channel impairments and impulsive noise and mitigate their effects in narrowband PLC systems. We examine ways to improve the communication performance based on current and emerging standards.

Index Terms

Channel modeling, impulsive noise, cyclostationary noise, narrowband PLC, power grid, power line channel, power line communications, Smart Grid.

M. Nassar, J. Lin, Y. Mortazavi, and B. L. Evans are with the Dept. of Electrical and Comp. Eng., The University of Texas, Austin, Texas USA. (see http://users.ece.utexas.edu/˜bevans/projects/plc/).

A. Dabak and I. Kim are with Texas Instruments Research and Development Center in Dallas, Texas USA.

Manuscript received September 6, 2011, resubmitted on January 20, 2012.

I. INTRODUCTION

Traditionally, a local utility has had to balance energy demand by local customers with energy supply. The energy supply came from power plants run by the local utility and/or the regional utility. Energy and information flowed only in one direction to the end user. In the future, a two-way flow of energy and information will occur throughout the Smart Grid.

The bidirectional flow of information will help the local utility manage the wide variety of types of power consumers and generators on the grid to guarantee quality of service while improving energy efficiency. To enable bidirectional flow of information, powerline communication (PLC) systems have been developed for use in every part of the grid. PLC systems may be placed in three bandwidth categories [1] as explained below.

Ultra narrowband (UNB), or very low frequency (VLF), PLC systems operate in the 0.3-3.0 kHz band to provide about 100 bps over ranges up to 150 km. An example, that has been deployed by many utilities, is the Two-way Automatic Communication System (TWACS) that sends two bits per mains cycle (i.e. 100 bps in Europe and 120 bps in North America). TWACS applications include automatic meter reading (AMR), outage detection, and voltage monitoring.

Narrowband (NB), or low frequency (LF), PLC systems operate in the 3-500 kHz band to deliver a few kbps in the single carrier case and up to 800 kbps in the multicarrier case. Several standards for commercial building automation, such as BacNet (ISO 16484-5) and LonTalk (ISO/IEC 14908-3), use single carrier NB-PLC. PRIME[1] and G3[2] are the well-known industry-developed multicarrier NB-PLC standards. Recently, ITU approved a family of standards that added G.hnem to the established PRIME and G3. These, in addition to the ongoing IEEE P1901.2 effort, extend the capabilities of local utilities into device-specific billing and smart energy management.

Broadband (BB), or high frequency (HF), PLC systems operate in the 1.8-250 MHz band to provide up to 200 Mbps for home area networks. The IEEE P1901 standard and the approved ITU G.996x recommendations (G.hn) are the most recent broadband standards. These systems are based on multicarrier communications. Furthermore, the first MIMO broadband PLC standard, using multiple available wires, was approved (Dec. 2011) as ITU Recommendation G.9963.

[1]PoweRline Intelligent Metering Evolution: http://www.prime-alliance.org

[2]http://www.maxim-ic.com/products/powerline/g3-plc

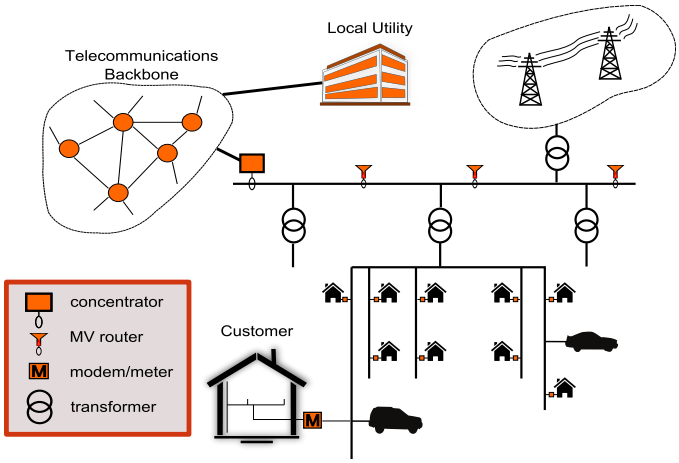

Fig. 1. Network-level system model for local utility powerline communications for US deployment: Meters transmit usage and load information on the LV access network through the transformer to a MV router. In turn, the MV router forwards this data to the concentrator that sends it to the utility company over a telecommunication backbone.

In the paper, we discuss narrowband PLC (NB-PLC) for local utility applications. A significant challenge in improving communication performance is overcoming channel distortion and noise. Channel distortion effects include the usual suspects of attenuation, frequency selectivity and fading due to the power transmission lines. They also include the effects of the transformer that bridges the low-voltage power line at the consumer with the medium voltage line for the local utility. Impulsive noise may be tens of deciBels higher than the background (thermal) noise. We model both the PLC channel and noise and show how current and emerging NB-PLC standards propose to deal with these impairments.

II. System Model of Local Utility PLC

PLC is envisioned as a platform for various Smart Grid applications. These applications include real-time monitoring and load balancing, improving grid robustness to disturbances, integrating alternate energy sources into the grid, and electric car charging and billing. Smart metering is currently one of the main target applications for PLC. Frequent meter readings of up to one read per 15 minutes per meter can provide the utility and the end user with better information about the load usage. The utility can use this information to optimize power generation and perform load management with finer time granularity. The users, on the other hand, can use this feedback to adjust their usage patterns to save on energy costs.

The basic system model for a utility PLC network for metering applications is given in Fig. 1.

The meter at the house collects usage information and sends this data across the low-voltage (LV) access network. Depending on the deployment environment, this information is aggregated at an LV router and passed through the transformer to an MV router (in Europe), or directly through the transformer to a medium-voltage (MV) router (in the US as shown in Fig. 1). Consequently, the MV routers forward the information to a concentrator that is connected to the utility company through a telecommunication backbone (such as WAN). While a bus topology is depicted in Fig. 1, other access topologies such as star and ring topologies are possible [2], [3]. Control data from the utility would flow in the opposite direction toward the customer.

III. Channel Models

In PLC systems, the electric grid constitutes the transmission medium. The signal propagates through electric wires and various discrete components such as transformers. In NB-PLC, the typical wire length in an LV or MV network is comparable to the propagation wavelength λ. For example, at $f = 500$ kHz, the typical wire length is greater or on the order of $\lambda/4 = \frac{\nu}{4f} \approx 100$m, where ν is the signal propagation speed. A TL of length $\lambda/4$ will cause a phase shift of π rads, and may give rise to a π-shifted reflected wave traveling in the opposite direction. As a result, the signal propagation is dominated by transmission line (TL) effects. Furthermore, the electrical length of power lines in NB-PLC networks is typically short enough to make the access impedance, determined by connected loads, dominate the characteristic impedances of the lines[3] at the input of PLC modems. These factors result in frequency selective channels with potentially deep notches that affect the communication performance of PLC systems. Fig. 2 shows examples of frequency selective responses and their corresponding root-mean-square (RMS) delay spreads encountered in the field. The RMS delay spread $\sigma_{\tau,\mu s}$ is a measure of the extent the channel is spread in time and is equal to the second central moment of the power delay profile. Additional loss is introduced when the signal passes through a transformer from the MV to the LV side. This is shown in Fig. 2 (4), where the channel has significantly higher attenuation than the other three cases. Next, we introduce two popular approaches for modeling PLC channels.

[3]The electrical length of a cable is its length expressed as the number of wavelengths of the propagating signal. As the electrical length tends to ∞, its reflected impedance approaches the characteristic impedance $Z_0(f)$ of the wire (this is the case in some broadband PLC systems).

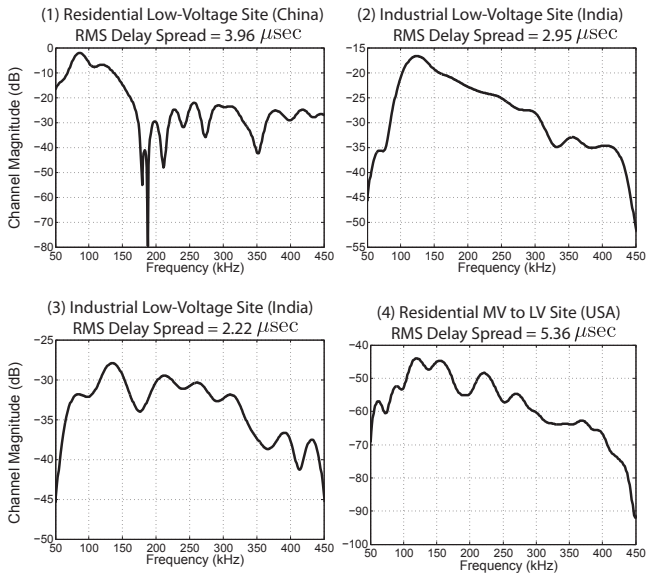

Fig. 2. Examples of different PLC channels in frequency domain and their corresponding RMS delay spreads.

A. Multi-Path Modeling

The multi-path model views the channel as an unknown function that needs to be estimated based on training data; hence, it does not use any prior information such as the network topology or component connections. Instead, it proposes a parametric model of the channel frequency response based on TL theory. This modeling approach is useful when the network topology is not available or an ad hoc deployment is desired. The multi-path model was first proposed in [4] and later augmented in [5]. It is based on the superposition of signal reflections at various loads predicted by TL theory. Its parametric form is given by

$$H(f) = \sum_{i=1}^{N} g_i e^{-\alpha(f) l_i} \times e^{-j2\pi f \tau_i} \tag{1}$$

where N is the number of propagation paths and g_i, $\alpha(f)$, l_i, τ_i are the gain, the attenuation factor, the length, and the delay of each path, respectively [5]. This modeling approach is illustrated in Fig. 3, where a sequence of training symbols is used to estimate the frequency response of the PLC channel. The accuracy of this model is highly dependent on N, the number of significant paths, with values between 15 to 44 required for a fit of a 110 m link [5]. The high number of parameters and the complex parameter estimation procedure are some of the disadvantages of this approach; however, the primary disadvantage is its inability to predict the channel response based on the PLC network topology and how it varies given a change in this topology. Furthermore,

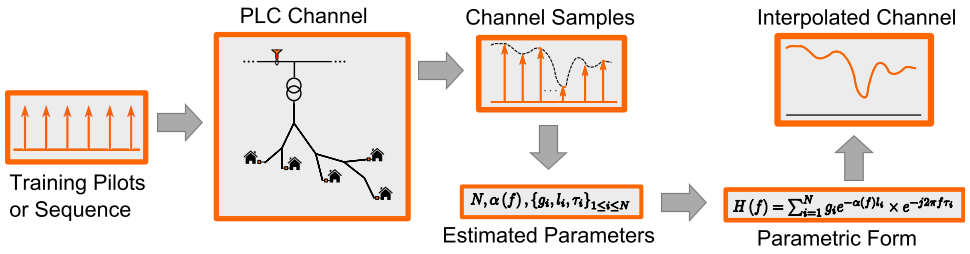

Fig. 3. The multi-path model approach: i) training symbols are sent over the channel, ii) the channel parameters are estimated, and iii) these parameters are used to interpolate the channel response at any frequency range using (1).

it is not clear how the model parameters change from site to site. This limits its applicability in coverage and deployment analysis for PLC systems.

On the other hand, the parametric form in (1) gives rise to a statistical description of the PLC channel if the parameters are viewed as random variables across different sites. An experimental and statistical analysis of such parameters for wireline channels is given in [6], where it is shown that the channel's average power gain $\bar{G}$ has a lognormal distribution. A random variable is said to be lognormal distributed if its logarithm is normally distributed. This usually arises in multiplication of *i.i.d.* random variables as in the channel gain of a PLC channel. Furthermore, a negative correlation between the RMS delay spread $\sigma_{\tau,\mu s}$ and $\bar{G}_{\text{dB}}$ is observed which could have an impact on the use of ISI-mitigation techniques. This correlation is modeled using a linear regression fit of the form

$$\log\left(\sigma_{\tau,\mu s}\right) = \theta \bar{G}_{\text{dB}} + \zeta \tag{2}$$

where the parameter fits for θ and ζ are provided for multiple practical wireline channels [6].

B. Transmission-Line Modeling

Transmission-line modeling, originally introduced for modeling DSL channels [7], views the channel as a deterministic quantity that is a function of the network topology and its electrical components. Two-conductor and multi-conductor transmission line models are two examples of bottom-up approaches using TL theory [7], [8]. In particular, a powerful approach is to model the electrical components of the PLC network as 2-port networks (2PN) and use these network parameters to relate the voltages and currents across the ports. ABCD parameters are particularly attractive due to the ease of their concatenation for different network topology configurations (simple matrix multiplications) [7]. Furthermore, using transmission line and circuit theory, the

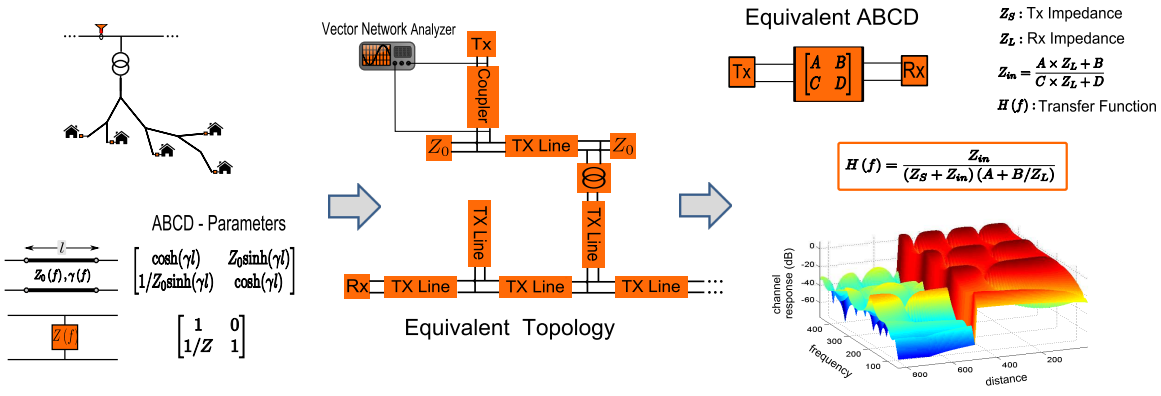

Fig. 4. The transmission line approach: i) the network topology is mapped to a tree of electrical components described by their ABCD models, then ii) the channel is estimated using the concatenation of ABCD parameters. A 3D figure of channel response vs. frequency vs. distance using transformer measurements can be generated and used in deployment studies. The huge dip in the channel gain is due to crossing the medium to low voltage through the transformer.

ABCD parameters of certain components such as shunt impedances and transmission lines can be calculated in closed form given the physical properties of the components. Other components commonly used in powerline networks, such as transformers and cap banks, that lack a physical model at the frequency range of interest need to be characterized using vector network analyzers. The overall approach of using TL modeling is illustrated in Fig. 4. A given powerline network, with its electrical components, is mapped onto an equivalent topology of ABCD parameters (or other network parameters). The equivalent ABCD between the desired TX-RX pair is computed and used to calculate the transfer function for that link. As Fig. 4 shows, this approach is generative since the topological aspects of the PLC-based network can be leveraged to compute the transfer function between any TX-RX pair in the network. The IEEE P1901.2 standard contributions given in [9] and [10] give a detailed analysis of using ABCD models to characterize channel responses of field data for an outdoor NB-PLC system. They also provide measured parameters for various components used in the field such as transformers and capacitor banks.

C. Time Varying Channels

Many electric devices connected to the power line network have a linear and time-invariant current-voltage relationship. As a result, they can be characterized by a static impedance. However, other devices exhibit nonlinear behavior that results in cyclic impedance properties with a period typically equal to half the AC mains cycle [11]. If these devices dominate the system's impedance,

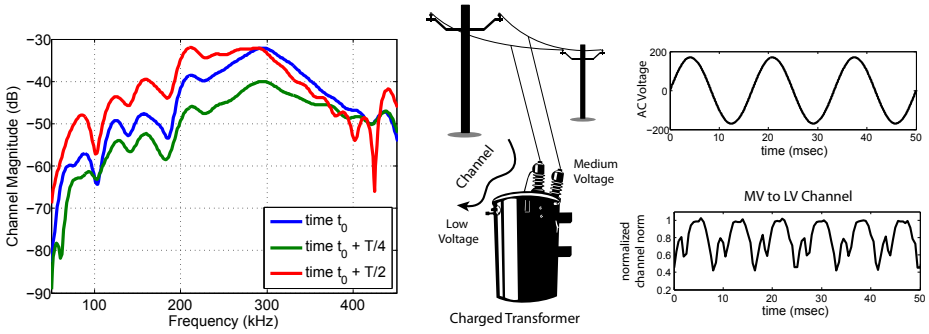

Fig. 5. The periodic time-varying channel of a charged transformer. The shape of the frequency response remains relatively constant while the channel norm varies periodically at a period $T = T_{AC}/2$. *[Transformer image was obtained from shutterstock.com]*

the channel will exhibit a time-varying cyclic behavior of the same period. For example, the channel across a charged transformer exhibits this periodic time-varying behavior which is shown in Fig. 5. This figure suggests a simple approximation for modeling the periodic channel of the transformer given by

$$h_T(t) = \alpha \left[\sin\left(\frac{4\pi}{T_{AC}} t\right) + \beta \right] h_0(t) \tag{3}$$

where α is a gain constant, β is a positive offset, and $h_0(t)$ is a common channel response. More general periodically time-varying channel models have been proposed in [11] and [6], while a discrete time-varying block channel model capturing this effect is proposed in [12]. On the other hand, random switching, connecting, and disconnecting devices from the network result in random load variations that lead to a form of time-selective fading.

IV. Noise Models

Powerline noise is a significant factor that contributes to the hostile environment observed in NB-PLC systems. This noise deviates significantly from the additive white Gaussian (AWGN) assumption typically used to design and analyze communication systems. Typical sources of PLC noise include: switching power supplies, silicon-controlled rectifiers, brush motors, dimmer switches and industrial sources directly connected to the supply network [3], [11]. The resulting noise is non-white with a time-varying spectral content that exhibits a $1/f$-type decay due to the decreasing concentration of noise sources with frequency and the used semiconductor devices.

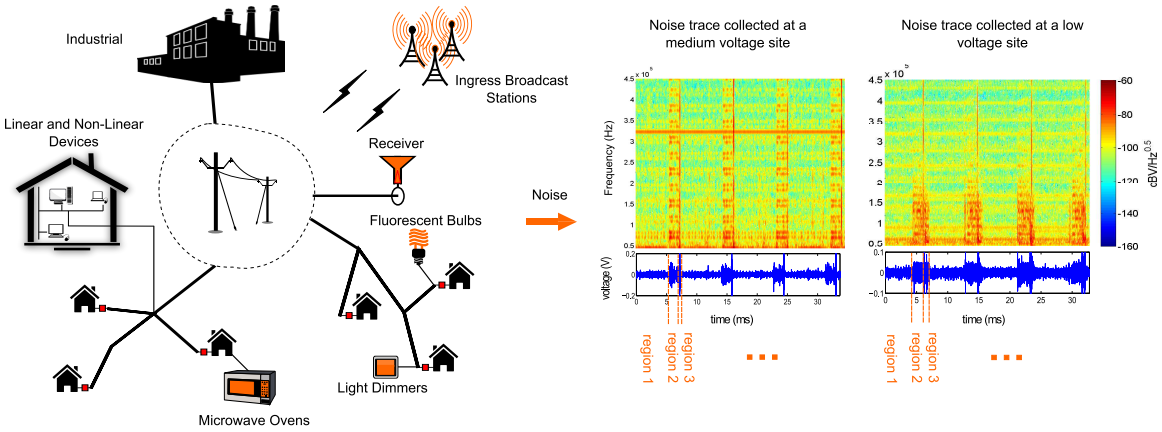

Fig. 6. A noise trace captured at a medium and low voltage field sites with some possible noise sources [9]. The noise exhibits cyclostationary features both in time and frequency domain. The trace can be divided into multiple regions in which the noise can be approximated by a stationary process with a given power and spectral shape [15].

A. Periodic and Cyclostationary Noise

Many empirical results on PLC noise properties have been reported in [13]. The noise was shown to have three main components: generalized background noise, periodic noise, and asynchronous impulsive noise. However, these studies address the noise in the 0.2-20 MHz range; thus, they are more applicable for broadband PLC systems.

More recently, studies targeted specifically for NB-PLC have shown that periodic noise and cyclostationary noise are the dominant components of the additive noise in these systems [3], [14]–[16]. A typical time-domain noise trace and a spectrogram of noise samples collected in the field at medium and low voltage sites with some possible sources is given in Fig. 6. Both traces, in addition to field data presented in the IEEE P1901.2 contribution given in [9], exhibit cyclostationarity in both the time and frequency domain. In [14], the authors propose to use a *cyclostationary* Gaussian model to characterize this aspect of the additive noise in NB-PLC systems. This model captures the temporal characteristics of the noise by a Guassian process with a time-varying variance that is periodic with a period equal to half the AC cycle; i.e.

$$n\left[k\right] \sim \mathcal{N}\left(0, \sigma^2\left[k\right]\right) \text{ with } \sigma^2\left[k\right] = \sigma^2\left[k + mT\right] \tag{4}$$

where $T = 0.5T_{AC} \times F_S$, T_{AC} is the duration of the AC cycle, F_S is the sampling frequency, and $m \in \mathbf{Z}$. Spectral coloring is introduced by passing this noise through a linear time-invariant shaping filter $h_s[k]$ with an exponentially decaying spectral density (see Fig. 7). A disadvantage

of this model is the complex parametric form used to characterize $\sigma^2[k]$ that leads to a data-intensive parameter estimation procedure. However, the primary disadvantage is that this model decouples the frequency and temporal shaping. As a result, a single spectral shape is used to shape the noise during each AC cycle which might not be appropriate when each region of the AC cycle has a different spectral shape (see Fig. 6 and Fig. 7). Since the main cyclostationarity captured is temporal, we refer to this model as the temporal cyclostationary model. In order to capture the cyclostationarity in both the time and frequency domain, the authors in [9] and [15] propose a novel cyclostationary model, which we refer to as spectro-temporal cyclostationary model. This model divides each noise period into M regions during which the noise is stationary (see Fig. 6). Each region is characterized by a spectral shape and a corresponding shaping filter. Using this model, the PLC noise is modeled as the convolution of an AWGN signal $s[k]$ with a linear periodically time-varying system $h[k,\tau]$ given by

$$n[k] = \sum_{\tau} h[k,\tau]s[\tau] = \sum_{i=1}^{M} \mathbf{1}_{k\in\mathcal{R}_i} \sum_{\tau} h_i[\tau]s[\tau] \tag{5}$$

where $\mathbf{1}_{\mathcal{A}}$ is the indicator function, and $h[k,\tau] = \sum_{i=1}^{M} h_i[\tau]\mathbf{1}_{k\in\mathcal{R}_i}$ for $0 \leq k \leq N-1$. This can be implemented using a filter bank as shown in Fig. 7. The linear time-invariant filters $h_i[k]$ correspond to spectral shaping filters for each region of the spectrogram in Fig. 6 and can be estimated using spectrum estimation techniques [15]. A comparison between the two modeling approaches is discussed in Fig. 7.

In addition to the cyclostationary noise, [16] shows that in the *very low frequency* (VLF), below 10 kHz, there is an additional wide-sense periodic noise component. Presently, the VLF range is extensively used by AMR providers. This periodic structure is exploited in [16] to filter out this component and increase the post-processing SNR of these systems.

B. Uncoordinated Interference

Powerline cables constitute a shared medium over which PLC operates. Due to this shared nature, PLC channels are potentially interference limited. As a result, recent increase in PLC standards and deployments has led to PLC coexistence issues [1], [3]. Interference from uncoordinated devices can lead to significant reductions in data rates and affect overall reliability. Uncoordinated transmissions could either result from other NB-PLC systems (deployed for other applications or a competing standard) or from broadband technologies used for in-home networking due to lack

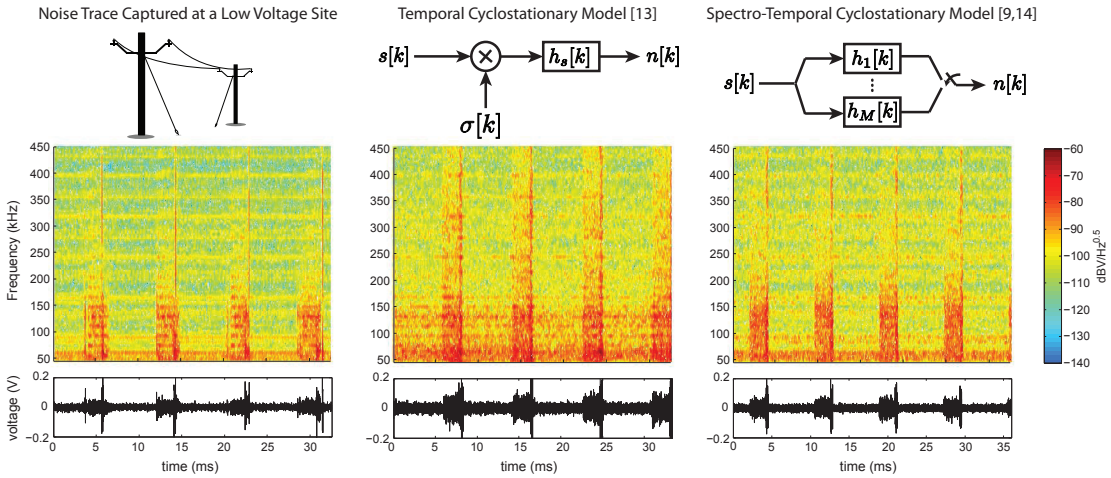

Fig. 7. The two cyclostationary noise models for NB-PLC: i) the temporal cyclostationary model [14] shapes an AWGN signal $s[k]$ by the temporal function $\sigma[k]$ and filters it through a single shaping filter $h_s[k]$, ii) the spectro-temporal cyclostationary model [15] filters an AWGN signal $s[k]$ by a filter bank of different shaping filters $h_i[k]$ each corresponding to a stationary region of the noise period. Since the temporal cyclostationary model is constrained to a single spectral shape, it overestimates the noise power spectral density in the $50-200$ kHz region by as much as 50 dBV/Hz. The spectro-temporal model provides a closer fit to the measured noise spectrogram.

of isolation. A time division multiple access (TDMA) approach, called Inter-System Protocol (ISP) [17], can provide coexistence between compliant standards such as IEEE 1901. An ISP stand-alone coexistence scheme is provided by G.9972. As a result, technologies that choose to implement it can coexist with IEEE 1901. However, there are already PLC technologies deployed in the field that do not implement ISP, particularly for metering applications, that are expected to have high deployment density. As a result, potential interference from these uncoordinated systems would be treated as noise at the receiver. Since uncoordinated transmission can be random and impulsive, it might not be fully captured by the noise models discussed above. This interference-based noise will be similar to *asynchronous* impulsive noise investigated in [13], [18] and will follow a Middleton Class-A or Gaussian mixture distribution.

In addition to uncoordinated PLC devices, there is interference from other uncoordinated man-made technologies such as broadcast stations over medium- and short-wave broadcast bands [13]. This interference is manifested as a strong additive narrowband noise observed in many field data such as the spectrogram of the medium voltage noise in Fig. 6 (at around 320kHz).

TABLE I

COMPARISON BETWEEN PLC AND WIRELESS ENVIRONMENTS

Wireless	**Narrowband PLC (3-500 kHz)**
Time selectivity of the channel is due to the node mobility.	Time selectivity results from random load variations due random switching, in the power grid.
The time-varying stochastic nature captured by its Doppler spectrum.	Time variation typically periodic with a period equal to half the AC mains [11] with lognormal time-selective fading [6].
Power decays as $d^{-\eta/2}$ where d is the distance and η is the propagation constant.	Power decays as $e^{-\alpha(f)d}$ along a powerline wire and is further attenuated when passing though transformers.
Additive noise is typically assumed stationary and Gaussian.	Additive noise is non-Gaussian and impulsive with a dominant cyclostationary component (see Section IV).
Dynamically changing propagation environment.	Some level of determinism provided by the fixed grid topology which can be exploited for deployment.
Typically interference limited.	Potentially interference limited by uncoordinated users due to increased deployment of different standards [1].
MIMO widely used such as in WiMAX and LTE.	MIMO of order (# of wires - 1) is possible (such as the G.9964 MIMO standard for BB-PLC).
Global synchronization across the network is difficult.	The AC main signal can simplify synchronization.

V. PLC CHANNELS VS. WIRELESS CHANNELS

The wireless communications field has seen tremendous developments that have completely transformed our way of life. Technologies such as digital modulation, digital signal processing (DSP), Orthogonal Frequency Division Multiplexing (OFDM), wireless networking, and Multiple-Input Multiple-Output (MIMO) systems have matured and became part of the standard communication toolset. The extent to which these tools can be leveraged for PLC depends largely on PLC channel conditions. For comparison, we contrast the two environments in Table I.

VI. COMMUNICATION TECHNIQUES

Previous sections describe the channel and noise conditions that exist in a typical PLC channel. Fig. 2 shows that the channel is typically better in the lower frequency ranges, while Fig. 6 suggests that the noise is higher in that frequency range. These conflicting quantities result in an

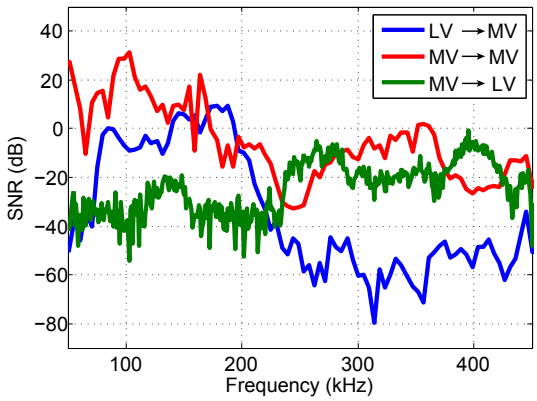

Fig. 8. The combined effect of the channel and noise: the SNR varies significantly from one site to another [19], [20]. It is not clear which band is the most suitable for transmission. In the MV→LV channel the higher frequency band would be more appropriate while for the other two channels the lower bands look more promising.

ambiguity about what frequency subband is the most appropriate for transmission. This is illustrated in Fig. 8 where we show the signal to noise ratio (SNR) for various PLC channels. In this section, we show how some of the widely used signal processing techniques for communications can be used for PLC and where their application needs to be tailored specifically for the PLC channel and the challenges it poses.

A. Multi-Carrier Modulation

Orthogonal frequency division multiplexing (OFDM) uses multiple orthogonal subcarriers to transmit data over frequency selective channels such as in Fig. 2. These are transformed into a collection of flat channels where each allows for a simple one-tap equalization. OFDM systems can provide the robustness needed to deal with varying PLC channels through water-filling based bit/power loading schemes. However, current narrowband PLC standards don't employ these algorithms due to their additional complexity. Instead, narrowband standards, such as G.hnem, employ tone mapping, a simpler version of water-filling [21]. A tone map specifies which tones will be loaded with bits versus which tones will be unloaded, or nulled, based on the SNR (see Fig. 8). Currently, the same number of bits is assigned to each loaded tone; however, unequal bit assignment is currently under investigation [21]. An additional benefit of OFDM is also its improved resilience to impulsive noise over single-carrier systems [22]. At the receiver, the discrete Fourier transform (DFT) spreads out the impulsive energy across all tones providing a

diversity effect that improves detection performance [22]–[24]. This is discussed in Section VI-C.

B. Coherent Vs. Non-Coherent Modulations

In an OFDM symbol, data can be modulated onto each subcarrier using coherent (e.g. PSK, QAM) or non-coherent (e.g. DPSK) modulation schemes. Evaluation of the performance of coherent vs. non-coherent detectors in various channel and noise conditions, as well as for different application scenarios, still remains an active research area. In general, the choice between coherent modulation and non-coherent modulation reflects complexity vs. performance tradeoffs. Non-coherent modulation relieves the receiver from the computationally expensive channel estimation and carrier frequency offset correction. Proper selection of the window length ensures that the channel phase distortion within it is approximately constant and thus is automatically canceled when subtracting the phases of two consecutive symbols. Assuming perfect channel estimation, the SNR gain of PSK over DPSK is generally 3 dB in AWGN. In non-Gaussian noise environments, the SNR loss of DPSK increases over 3 dB as the noise becomes more impulsive [25]. This is because the occurrence of high amplitude noise impulses can result in noisy phase reference and severe error propagation. On the other hand, the performance of non-coherent coded modulation can be improved by increasing the receiver complexity. In [26], the authors proposed a non-coherent maximum likelihood sequence estimator (NMLSE) using overlapped observation blocks. In AWGN, by increasing the observation length, the performance of the non-coherent coded modulation with NMLSE converges to that of the coherent coded modulation with the Viterbi decoder. However, such performance gain is significantly suppressed due to the presence of impulsive noise [27].

C. Impulsive Noise Mitigation

In highly impulsive noise environments, the decrease of subchannel SNR can be too severe to be mitigated by forward error correction (FEC) and interleaving. In this situation, denoising algorithms can be used to remove the impulsive noise from the received signal before passing it to the detector. These methods generally utilize the sparse structure of the impulsive noise. Two compressed sensing (CS) algorithms were described in [23] and [24]. These methods utilize the information contained in the null tones of an OFDM symbol to cancel out sufficiently sparse but strong impulse noise. Recently, two sparse Bayesian learning (SBL) methods were proposed

for impulsive noise mitigation in OFDM systems [28]. The methods utilize information either on the known subcarriers, such as null tones and pilots, to cancel out impulsive noise or on all subcarriers to perform joint estimation-detection of impulse noise and data symbols. In addition, these algorithms can be augmented using statistical models of the impulse noise to boost the detection performance significantly over the CS methods.

VII. Current Standards

PRIME and G3 are the well-known industry-developed OFDM-based narrowband PLC standards. Both operate in the CENELEC-A (CEN A) band from 3 to 95 kHz (ITU-T G.9955/G.9956 and IEEE P1901.2 extend G3 to the FCC band from 159.4 to 478.1 kHz), and adopt non-coherent modulation (i.e. DPSK) in combination with forward error correction (FEC) coding (e.g. convolutional coding (Conv) and Reed-Solomon coding (RS)) to combat adverse channel impairments and noise scenarios. Details about both standards and the comparisons between them are well-described in [29] and [30]. PRIME and G3 PLC modems have been developed by several companies, and have demonstrated success in field trials [31], [32].

To resolve the interoperability issues among the existing technologies, unified international standards have been developed for the next generation narrowband PLC technology. The very recently approved ITU-T Recommendations G.9955 and G.9956 specify the physical layer (PHY) and the data link layer (DLL), respectively, of G.hnem and document PRIME and G3 to facilitate the transient period [21]. Similarly, IEEE P1901.2 is being developed to provide advanced features based on G3. Both these standards enable scalable data rates up to 500 kbps over a portion of the CENELEC band (3–95 kHz in CEN A, 95–125 kHz in CEN B and 125–148.5 kHz in CEN CD) and the entire US Federal Communications Commission (FCC) band (34.375–487.5 kHz). Some PHY layer parameters of these two new standards are listed in Table II and compared to those of PRIME and G3. Note that since the PHY specifications of PRIME and G3 are defined in baseband real-valued settings, the FFT length is twice the number of subcarriers, whereas IEEE P1901.2 and G.hnem are specified in complex OFDM settings, where the FFT length is equal to the number of subcarriers. The maximum data rates take into account of cyclic prefix (CP), forward error correction (FEC) coding, and the overhead of frame control headers, preambles, channel estimation symbols and pilots.

TABLE II

PHYSICAL LAYER PARAMETERS OF PRIME, G3, IEEE P1901.2 AND G.HNEM.

Parameter		PRIME	G3	IEEE P1901.2	G.hnem
Frequency Range	CEN A	42–89 kHz	35.9–90.6 kHz	35.9–90.6 kHz	35.9–90.6 kHz
	FCC	/	159.4–478.1 kHz	35.9–487.5 kHz	34.4–478.1 kHz
Sampling Frequency	CEN A	250 kHz	400 kHz	400 kHz	200 kHz
	FCC	/	1.2 MHz	1.2 MHz	800 kHz
FFT Length	CEN A	512	256	256	128
	FCC	/	256	256	256
Cyclic Prefix (Duration)	CEN A	48 (192μs)	30 (75μs)	30 (75μs)	20/32 (100μs/160μs)
	FCC	/	30 (25μs)	30 (25μs)	40/64 (50μs/80μs)
Window Size	CEN A	0	8	8	8
	FCC	/	8	8	16
Effective CP (Duration)	CEN A	48 (192μs)	22 (55μs)	22 (55μs)	12/24 (60μs/120μs)
	FCC	/	22 (18.3μs)	22 (18.3μs)	24/48 (30μs/60μs)
Subcarrier Spacing	CEN A	488 Hz	1.5625 kHz	1.5625 kHz	1.5625 kHz
	FCC	/	4.6875 kHz	4.6875 kHz	3.125 kHz
OFDM Duration	CEN A	2240μs	695μs	695μs	700/760μs
	FCC	/	231.7μs	231.7μs	350/380μs
Modulation[4]		DPSK M=2,4,8	DPSK M=2,4,8	DPSK (QAM) M=2,4,8,16	QAM M=2,4,8,16
FEC		Conv (Optional)	Conv+RS	Conv+RS	Conv+RS
Maximum Data Rate	CEN A	61.4/123 kbps[5]	45 kbps	52.3 kbps	101.3 kbps
	FCC	/	207.6 kbps	203.2/207.6 kbps[6]	821.1 kbps

The comparison of modulation schemes among the standards in Table II reveals a new trend that favors coherent over non-coherent modulation used in PRIME and G3. In particular, coherent modulation is optional in IEEE P1901.2 and mandatory in G.hnem. The purpose is to guarantee higher data rates and reliable communication [21], [27], and provide potential support for in-home PLC applications. As discussed in the Section VI-B, coherent detection could significantly improve receiver's sensitivity and robustness, especially in the presence of impulsive noise. However, it generally requires higher complexity for channel estimation. For example, in the optional coherent modulation modes in IEEE P1901.2, two preamble symbols are added after

[4]For IEEE P1901.2, coherent modulation with BPSK/QPSK/8PSK/16-QAM is optional. M is the constellation size.

[5]With the optional convolutional coding turned on and off, respectively.

[6]For coherent and non-coherent modulations, respectively.

the frame control header (FCH) for channel estimation. An additional feature of IEEE P1901.2 is that, unlike G.hnem, it provides an optional adaptive multi-tone mask for the preamble and header. This allows for PHY/MAC protocols that facilitate reliable communication for MV/LV crossing in the US grids demonstrated in various field tests [33].

VIII. Deployment and Challenges

The vast majority of today's deployments are based on frequency shift keying (FSK) and Spread-FSK as specified in the IEC 61334 standard. These low data rate NB-PLC technologies provide 1.2-2.4 kbps with high robustness. However, as the data rate required by Smart Grid applications increases, so does the interest in deploying high data rate OFDM-based PLC technologies such those discussed in Section VII. While the verdict on which standard will dominate is still out, the likely answer will depend on the deployment environment, regulations, and the specific application. Here we review some of the deployment aspects and challenges.

A. Deployment Enviroment

Topological characteristics of power grids have been studied in [1], [34]. Characteristics such as connectivity, clustering, and average node degrees can provide a better understanding of the power grid as a communication network. For example, [1] analyzes an MV rural network and shows that due to its low connectivity it is prone to become disconnected under node failure. More study cases across the world are necessary to gain a good statistical model for different grids both on the MV and LV sites. This in turn will provide intuition about network design and robustness (such as designing hybrid PLC/wireless networks). Without this statistical modeling of world-wide grid statistics, we approach deployment from the perspective of meter density per transformer and the deployment enviroment.

In rural deployments, the number of households per meter on the LV side of the MV/LV transformer will typically be small (in the range of $< 5 - 10$). In this case, it is not economical to have a concentrator on the low voltage (LV) side of the transformer. Similarly, the desired range for reaching the household meters can be large, on the order of several miles especially in countries like USA and Europe. In [35], it was reported that with an attenuation of 3-5 dB per km at $\sim$100 kHz and up to 6-8 dB per km in higher frequency range of $\sim$ 400 kHz, achieving these long distances of tens of kms for rural applications may be challenging for PLC technologies

employing the 50-500 kHz frequencies. Typically, the UNB technologies such as TWACS can be used for these deployments. For semi-rural applications in the USA, the number of LV meters per transformer is still approximately 5-10, while the distances are smaller in the range of 3-5 km with a higher meter density. In this case, technologies designed for crossing the MV/LV transformers should be used for deployment. Field trials have confirmed that G3 is capable of crossing the transformer in both directions [32]. Although awaiting empirical verification, by design one would expect that P1901.2 and G.hnem to achieve this as well making them valid deployment candidates. On the other hand, for urban deployments with very high user density, the number of LV side nodes is larger in the range of 100 to also 1000 in Spain/France. In this case, it is economical to have a concentrator on the low voltage side of the transformer and PLC technologies like PRIME/G3/IEEE P1901.2/G.hnem can be used for deployment.

B. Throughput Requirements and Standards Coexistence

Rural applications, with a low household density per square km, typically require low data rates in the order of few 100 bps. On the other hand, semi-rural and urban applications, due to the higher density of households, require higher data rates in the tens of kbps range. In addition, an accurate estimate of data rates needed for various Smart Grid application is still an open problem and will need to take into account the high correlation in the collected data [1].

Also, as highlighted in Section IV-B, the coexistence of different PLC standards is a growing problem. With the widespread adoption of PLC technology, interference from uncoordinated users could prove to be a bottleneck in communication performance.

IX. Conclusion

In this article, we characterize the channel and the additive noise of a medium that was primarily designed for one-directional flow of power at a main frequency of 50 or 60 Hz. NB-PLC systems use some or all of the 3 to 500 kHz band. Power transmission lines exhibits attenuation, frequency selectivity, and fading. Additional nonlinear and linear impairments are due to the transformer. Cyclostationary noise forms the dominant component of noise in these systems. We conclude by showing how to mitigate channel impairments and additive noise given models for them, esp. in the context of current and emerging single carrier and multicarrier NB-PLC standards. In general, PLC systems are attractive because they can be deployed over existing power lines.

NB-PLC systems, in particular, enable two-way communication links between customer sites and a monitoring and control center at the local utility. Such links form a key component for intelligently monitoring and controlling energy flows in the future Smart Grid, enabling improved efficiency and reliability of power delivery.

ACKNOWLEDGMENT

The authors would like to express thanks for Aclara and Mr. Gordon Gregg for their support and facilitation of the experiments where the data was collected. Furthermore, the authors extend their thanks to Dr. Stefano Galli and the paper reviewers for their feedback that helped make this article accurate and up-to-date with the latest standard developments. In addition, Mr. Nassar, Ms.Lin, Mr. Mortazavi, and Prof. Evans were supported by the Semiconductor Research Corporation under GRC ICSS Task ID 1836.063. Last, the authors would like to acknowledge the use of clip art in the public domain from the *OpenClipArtLibrary* project in parts of Figures 1, 5, 6, and 7.

REFERENCES

[1] S. Galli, A. Scaglione, and Z. Wang, "For the grid and through the grid: The role of power line communications in the smart grid," *Proc. IEEE*, vol. 99, no. 6, pp. 998–1027, 2011.

[2] H. Hrasnica, A. Haidine, and R. Lehnert, *Broadband Powerline Communications : Network Design*, 2005.

[3] H. C. Ferreira, L. Lampe, J. Newbury, and T. G. Swart, Eds., *Power Line Communications: Theory and Applications for Narrowband and Broadbank Communications over Power Lines*. Wiley, 2010.

[4] H. Philipps, "Modeling of powerline communication channels," *Proc. Int. Symp. Power Line Commun. and Its Appl.*, pp. 14–21, 1999.

[5] M. Zimmermann and K. Dostert, "A multipath model for the powerline channel," *IEEE Trans. Commun.*, vol. 50, no. 4, pp. 553–559, 2002.

[6] S. Galli, "A novel approach to the statistical modeling of wireline channels," *IEEE Trans. on Commun.*, vol. 59, no. 5, pp. 1332–1345, 2011.

[7] T. Banwell and S. Galli, "A new approach to the modeling of the transfer function of the power line channel," *Proc. Int. Symp. Power Line Commun. and Its Appl.*, pp. 319–324, 2001.

[8] O. Hooijen, "On the relation between network-topology and power line signal attenuation," *Proc. Int. Symp. Power Line Commun. and Its Appl.*, pp. 45–56, 1998.

[9] A. Dabak, B. Varadrajan, I. H. Kim, M. Nassar, and G. Gregg, *Appendix for noise channel modeling for IEEE P1901.2*, IEEE P1901.2 Std., June 2011, doc: 2wg-11-0134-05-PHM5.

[10] V. Borisov and P. Chiummiento, *Impedance Variation Impairment on OFDM PLC PHY*, IEEE P1901.2 Std., January 2011, doc: 2wg-11-0010-01-PHM5.

[11] F. Canete, J. Cortes, L. Diez, and J. Entrambasaguas, "Analysis of the cyclic short-term variation of indoor power line channels," *IEEE J. Sel. Areas Commun.*, vol. 24, no. 7, pp. 1327–1338, 2006.

[12] S. Galli and A. Scaglione, "Discrete-time block models for transmission line channels: Static and doubly selective cases," *IEEE Trans. Commun.*, September 2011, submitted, available online: http://arxiv.org/abs/1109.5382.

[13] M. Zimmermann and K. Dostert, "Analysis and modeling of impulsive noise in broad-band powerline communications," *IEEE Trans. Electromagn. Compat.*, vol. 44, no. 1, pp. 249–258, 2002.

[14] M. Katayama, T. Yamazato, and H. Okada, "A mathematical model of noise in narrowband power line communication systems," *IEEE J. Sel. Areas in Commun.*, vol. 24, no. 7, pp. 1267–1276, 2006.

[15] M. Nassar, A. Dabak, I. H. Kim, T. Pande, and B. L. Evans, "Cyclostationary noise modeling in narrowband powerline communication for smart grid applications," *Proc. IEEE Int. Conf. on Acoustics, Speech, and Signal Process.*, pp. 3089–3092, March 2012.

[16] D. Rieken, "Periodic noise in very low frequency power-line communications," *Proc. IEEE Int. Symp. Power Line Commun. and Its Appl.*, pp. 295–300, 2011.

[17] S. Galli, A. Kurobe, and M. Ohura, "The inter-PHY protocol (IPP): A simple coexistence protocol for shared media," *Proc. IEEE Int. Symp. Power Line Commun. and Its Appl.*, pp. 194–200, 2009.

[18] M. Nassar, K. Gulati, Y. Mortazavi, and B. L. Evans, "Statistical modeling of asynchronous impulsive noise in powerline communication networks," *Proc. IEEE Int. Global Commun. Conf.*, pp. 1–6, December 2011.

[19] D. Rieken, D. Langenberg, M. Walker, G. Gregg, I. H. Kim, A. Dabak, and T. Pande, *Channel and Noise Measurements In The US Rural Grid New Results With Improved Coupler and Measurement Procedure*, IEEE P1901.2 Std., April 2011, doc: 2wg-11-0086-00-PHM5.

[20] ——, *Channel and Noise measurements*, IEEE P1901.2 Std., April 2011, doc: 2wg-11-0124-00-PHM5.

[21] V. Oksman and J. Zhang, "G.HNEM: the new ITU-T standard on narrowband PLC technology," *IEEE Commun. Mag.*, vol. 49, no. 12, pp. 36–44, 2011.

[22] J. Haring, *Error Tolerant Communication over the Compound Channel*. Shaker-Verlag, Aachen, 2002.

[23] G. Caire, T. Al-Naffouri, and A. Narayanan, "Impulse noise cancellation in OFDM: an application of compressed sensing," in *Proc. IEEE Int. Sym. on Inf. Theory*, 2008, pp. 1293–1297.

[24] L. Lampe, "Bursty impulse noise detection by compressed sensing," *Proc. IEEE Int. Symp. Power Line Commun. and Its Appl.*, pp. 29–34, 2011.

[25] H. Huynh and M. Lecours, "Impulsive noise in noncoherent M-ary digital systems," *IEEE Trans. Commun.*, vol. 23, no. 2, pp. 246–252, 1975.

[26] D. Raphaeli, "Noncoherent coded modulation," *IEEE Trans. Commun.*, vol. 44, no. 2, pp. 172–183, 1996.

[27] D. Umehara, M. Kawai, and Y. Morihiro, "Performance analysis of noncoherent coded modulation for power line communications," *Proc. Int. Symp. Power Line Commun. and Its Appl.*, pp. 291–298, 2001.

[28] J. Lin, M. Nassar, and B. L. Evans, "Non-parametric impulsive noise mitigation in OFDM systems using sparse Bayesian learning," in *Proc. IEEE Int. Global Commun. Conf*, 2011, pp. 1–5.

[29] M. Hoch, "Comparison of PLC G3 and PRIME," *Proc. IEEE Int. Symp. Power Line Commun. and Its Appl.*, pp. 165–169, 2011.

[30] I. H. Kim, B. Varadarajan, and A. Dabak, "Performance analysis and enhancements of narrowband OFDM powerline communication systems," in *Proc. IEEE Int. Conf. on Smart Grid Commun.*, 2010, pp. 362–367.

[31] A. Aruzuaga, I. Berganza, A. Sendin, M. Sharma, and B. Varadarajan, "PRIME interoperability tests and results from field," in *Proc. IEEE Int. Conf. on Smart Grid Commun.*, 2010, pp. 126–130.

[32] K. Razazian, M. Umari, A. Kamalizad, V. Loginov, and M. Navid, "G3-PLC specification for powerline communication: Overview, system simulation and field trial results," *Proc. IEEE Int. Symp. Power Line Commun. and Its Appl.*, pp. 313–318, 2010.

[33] B. Varadarajan, I. H. Kim, A. Dabak, D. Rieken, and G. Gregg, "Empirical measurements of the low-frequency power-line communications channel in rural North America," *Proc. IEEE Int. Symp. Power Line Commun. and Its Appl.*, pp. 463–467, 2011.

[34] Z. Wang, A. Scaglione, and R. Thomas, "Generating statistically correct random topologies for testing smart grid communication and control networks," *IEEE Trans. Smart Grid*, vol. 1, no. 1, pp. 28–39, 2010.

[35] A. Dabak, B. Varadarajan, I. H. Kim, V. Olson, and S. McHann, *MV/LV communication modeling using S-parameter/ABCD parameters*, IEEE P1901.2 Std., March 2011, doc: 2wg-11-070-00-PHM5.

Marcel Nassar (mnassar@utexas.edu) received a B.E. degree in computer and communications engineering, with a minor degree in mathematics, from the American University of Beirut in 2006, and an M.S. degree in electrical and computer engineering from The University of Texas at Austin in 2008, where he is currently pursuing a PhD degree. His interests lie at the intersection of signal processing and machine learning with application to statistical modeling and mitigation of interference in communication systems.

Jing Lin (linj@mail.utexas.edu) received a B.S. degree in electrical engineering in 2008 from Tsinghua University, China, and an M.S. degree in electrical and computer engineering in 2010 from the University of Texas at Austin, where she is currently pursuing a PhD degree. Her research has been focused on signal processing algorithms and implementations for powerline communications.

Yousof Mortazavi (ymortazavi@mail.utexas.edu) received his B.S. from the University of Tehran, Iran in 2005. In 2006, he joined the Electrical and Computer Engineering Department at The University of Texas at Austin and was awarded the M.S. in 2008. Currently he is working towards his Ph.D. at the same department. His interests are signal processing for communication systems and calibration and digital post-processing in mixed-signal integrated circuits, specifically for data converters.

Anand Dabak (dabak@ti.com) received the B.Tech. degree in electrical engineering from the Indian Institute of Technology, Bombay, India in 1987 and the M.Sc. and Ph.D. degrees in EE, from Rice University, Houston, TX, in 1989 and 1992. He joined Texas Instruments Incorporated, Dallas, TX, in 1995 and has since then worked on the algorithm issues related to wireless and power line communications (PLC). He has been involved in the standardization activity and development in Bluetooth, ultra-wideband, digital video broadcasting-handheld and 3rd Generation Partnership Project wideband code division multiple access, and long-term evolution. Currently he is TI -Fellow and working on power line communication (PLC) and other problems in Smart Grid.

Il Han Kim (il-han-kim@ti.com) received the B.S. and M.S. degrees in electrical engineering from Korea Advanced Institute of Science and Technology in 2002 and 2004, respectively, and Ph.D. degree in electrical engineering from Purdue University in 2008. During 2004 and 2005, he was with the Electronics and Telecommunications Research Institute, Daejeon, Republic of Korea. Since January 2009, he has been with the Systems and Applications R&D Center, Texas Instruments Incorporated, where he has been working on power line communications. His research interests include the analysis of various communication systems.

Brian L. Evans (bevans@ece.utexas.edu) received a B.S. degree in electrical engineering and computer science from the Rose-Hulman Institute of Technology in 1987 and M.S. and Ph.D. degrees in electrical engineering from the Georgia Institute of Technology in 1988 and 1993, respectively. From 1993 to 1996, he was a post-doctoral researcher at the University of California, Berkeley. Since 1996, he has been a faculty member in electrical and computer engineering at The University of Texas at Austin. He currently holds the Engineering Foundation Professorship. In 1997, he won the U.S. NSF CAREER Award. He is a Fellow of the IEEE.